DBD NMEs by interacting shell model

岩田順敬（関西大学）
Yoritaka Iwata (Kansai University)

Ref.) **Y. Iwata, N. Shimizu et al. Phys. Rev. Lett. 2016**
J. Terasaki, Y. Iwata, Phys. Rev. C 2019
S. Sarkar, Y. Iwata, P. K. Raina, Phys. Rev. C 2020

Contents

- Shell model research [overview]

- Shell model calculation for DBD of Ca48
 - Large scale calculation by Tokyo group -

- Right handed weak boson ?

- Summary

Next occasion:
Heavy “sterile neutrino” (right-handed neutrino) ?

Recent trend on ISM calculations: ①"more structure" = new paths

PRL 113, 262501 (2014) PHYSICAL REVIEW LETTERS week ending 31 DECEMBER 2014

Nuclear Structure Aspects of Neutrinoless Double-β Decay

B. A. Brown,[1] M. Horoi,[2] and R. A. Sen'kov[2,3]
[1]Department of Physics and Astronomy and National Superconducting Cyclotron Laboratory, Michigan State University, East Lansing, Michigan 48824-1321, USA
[2]Department of Physics, Central Michigan University, Mount Pleasant, Michigan 48859, USA
[3]Department of Natural Sciences, LaGuardia Community College, The City University of New York, Long Island City, New York 11101, USA

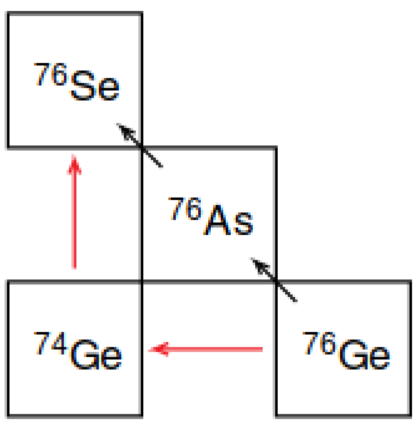

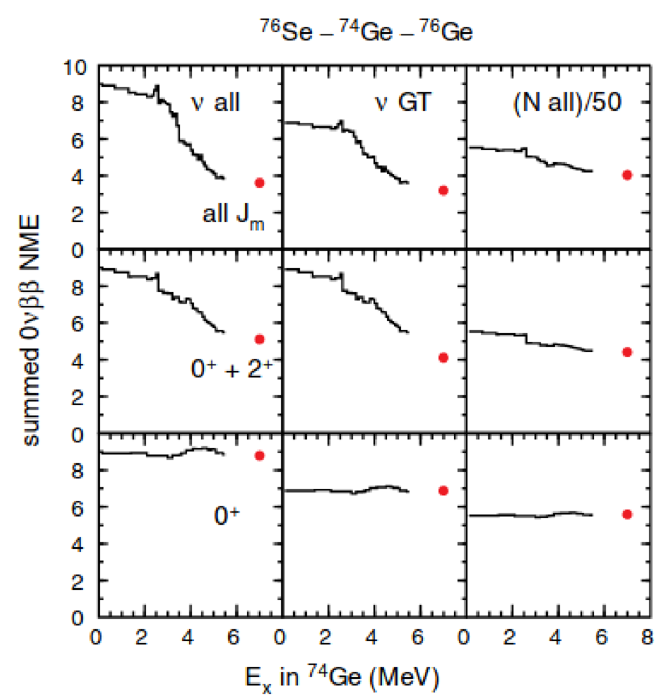

→ **DGT**, **2ν**, **0ν**

Experiments

At the same time

Neacsu, Horoi, Phys. Rev. C, 2018

Recent trend on ISM calculations: ②Hadronic current by EFT

PHYSICAL REVIEW C **98**, 035502 (2018)

Shell model study of using an effective field theory for disentangling several contributions to neutrinoless double-β decay

Mihai Horoi* and Andrei Neacsu†
Department of Physics, Central Michigan University, Mount Pleasant, Michigan 48859, USA

[λ mechanism] see also ... Simkovic et al., Front Phys. 2017

$$\left[T^{0\nu}_{1/2}\right]^{-1} = G_{01} g_A^4 \left| \eta_{0\nu} M_{0\nu} + \left(\eta^{L}_{N_R} + \eta^{R}_{N_R}\right) M_{0N} + \eta_{\tilde{q}} M_{\tilde{q}} + \eta_{\lambda'} M_{\lambda'} + \eta_{\lambda} X_{\lambda} + \eta_{\eta} X_{\eta} \right|^2 .$$

the left-right symmetric model
with R-parity-violating SUSY model

Ordinary case

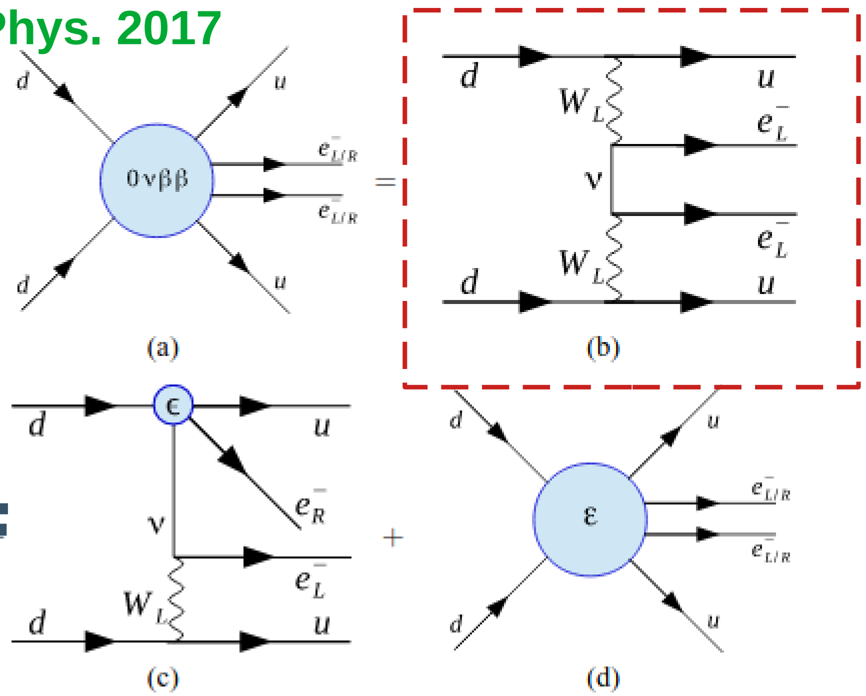

→ for contributions of ν_L , ν_R, W_L , W_R

Recent trend on ISM+ calculations: ③Ab-initio (IMSRG usable for ISM)

PHYSICAL REVIEW LETTERS **124,** 232501 (2020)

***Ab Initio* Treatment of Collective Correlations and the Neutrinoless Double Beta Decay of ^{48}Ca**

J. M. Yao,[1,*] B. Bally,[2,†] J. Engel,[2,‡] R. Wirth,[1,§] T. R. Rodríguez,[3,‖] and H. Hergert[1,4,¶]
[1]*Facility for Rare Isotope Beams, Michigan State University, East Lansing, Michigan 48824-1321, USA*
[2]*Department of Physics and Astronomy, University of North Carolina, Chapel Hill, North Carolina 27516-3255, USA*
[3]*Departamento de Física Teórica y Centro de Investigación Avanzada en Física Fundamental, Universidad Autónoma de Madrid, E-28049 Madrid, Spain*
[4]*Department of Physics & Astronomy, Michigan State University, East Lansing, Michigan 48824-1321, USA*

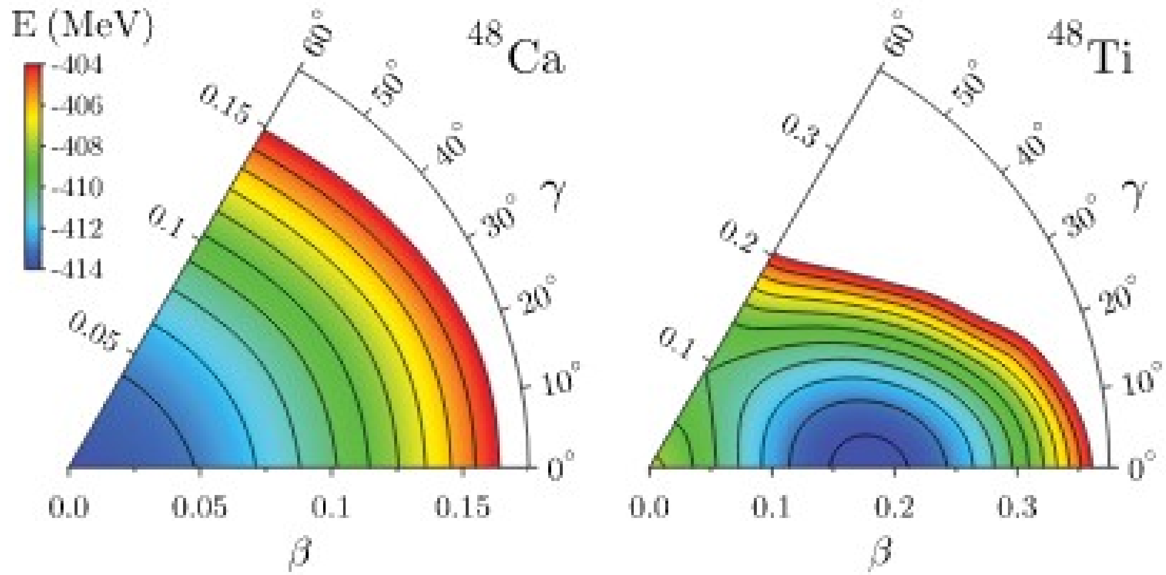

$M^{0\nu} = 0.61$

GCM

Large scale ISM calculations Including 2 major shells (Tokyo)

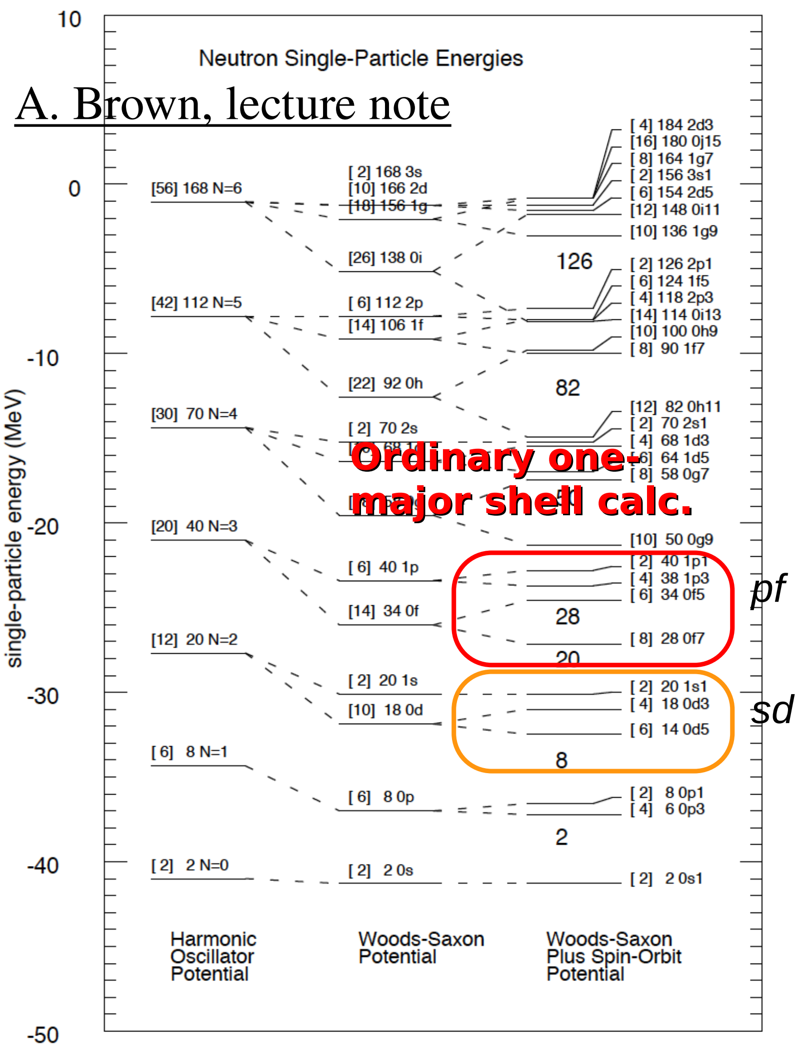

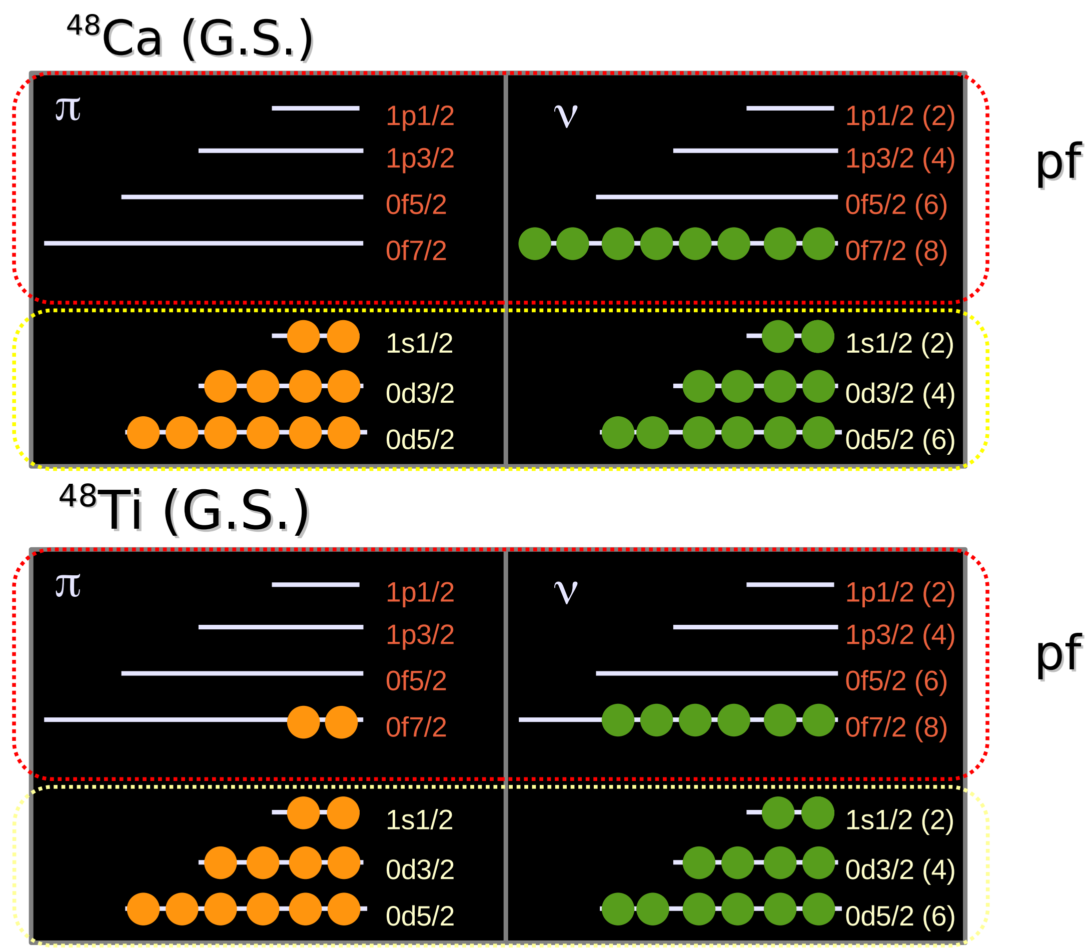

1) Adjustment of interaction for “double beta decays”

[EXPERIMENT] F. Videbaek *et al.*, NPA (1986)
2nd 0^+ state of ^{48}Ca was pointed out to be proton-excitation state

proton excitation included in 2nd 0^+ state of ^{48}Ca:

1 shell GXPF1B: 0.00

2 shells $\boxed{\text{SDPFMU: 0.22}}$

Proton excitation number

^{48}Ca (G.S.)

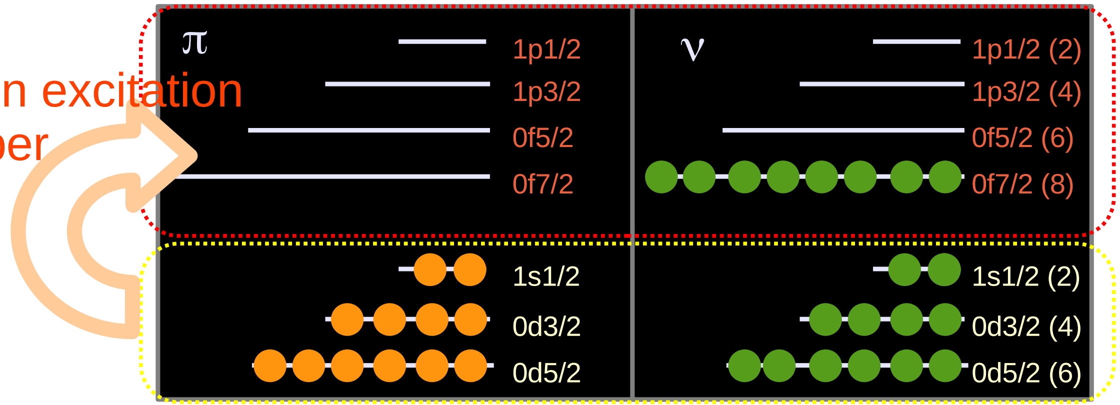

“0.22” is still too small to be pronounced as the proton-excitation state
cf.) the parity difference between the *sd*- and *pf*- orbits.

Our idea is to adjust the gap between the *sd*- and *pf*- shells
to reproduce the experimental excitation energy of 2nd 0^+ state of ^{48}Ca

2) Shell gap

[EXPERIMENT] F. Videbaek *et al.*, NPA (1986)
2nd 0^+ state of ^{48}Ca was pointed out to be proton-excitation state

By reducing the shell gap of Ca40 about 2MeV → 5.8 MeV
Slightly modified interaction SDPFMU-db made from SDPFMU

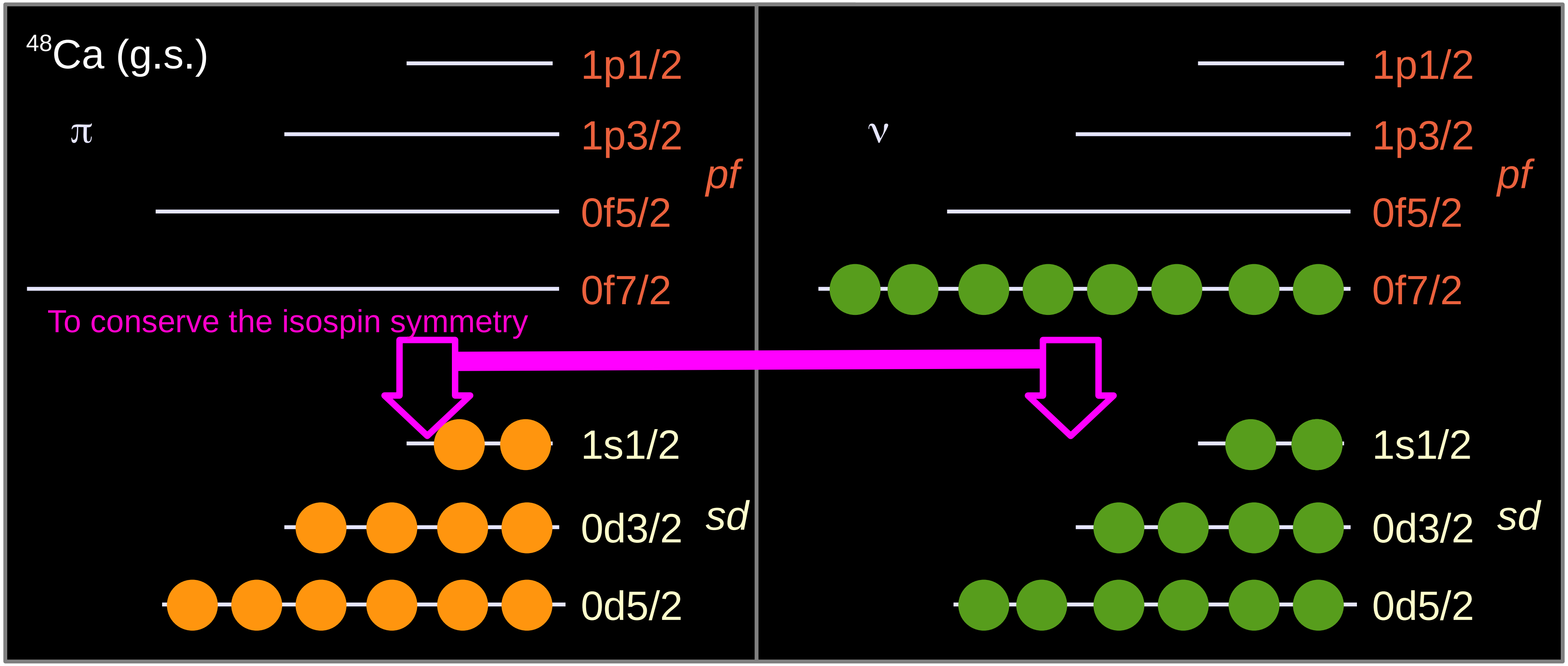

Energy spectra, as a test of the nuclear structure calculation

As an evidence of good description,
the energy spectra made by SDPFMU-db is compared to the experiment;
SDPFMU-db is an effective interaction made for 2 major shell description.

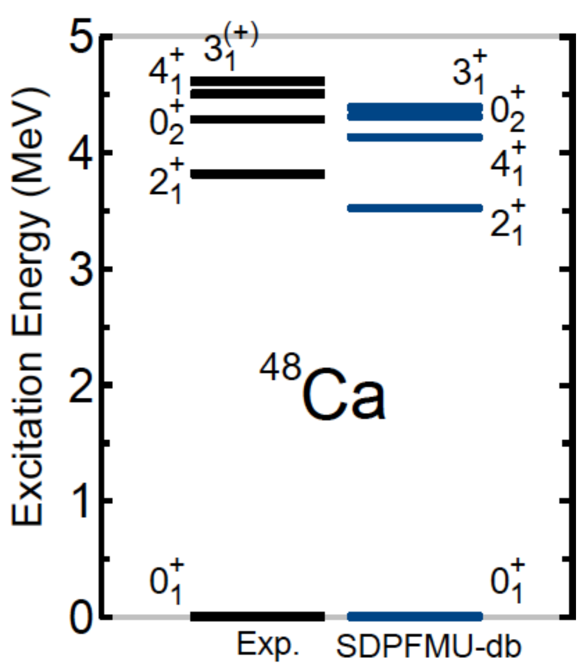

2hw component ratio

SDPFMU-db
Ca48 (g.s.) , Ti48 (g.s.): 22%, 33%

Two neutrino process

[Experiment]: Yako *et al.* PRL (2009)

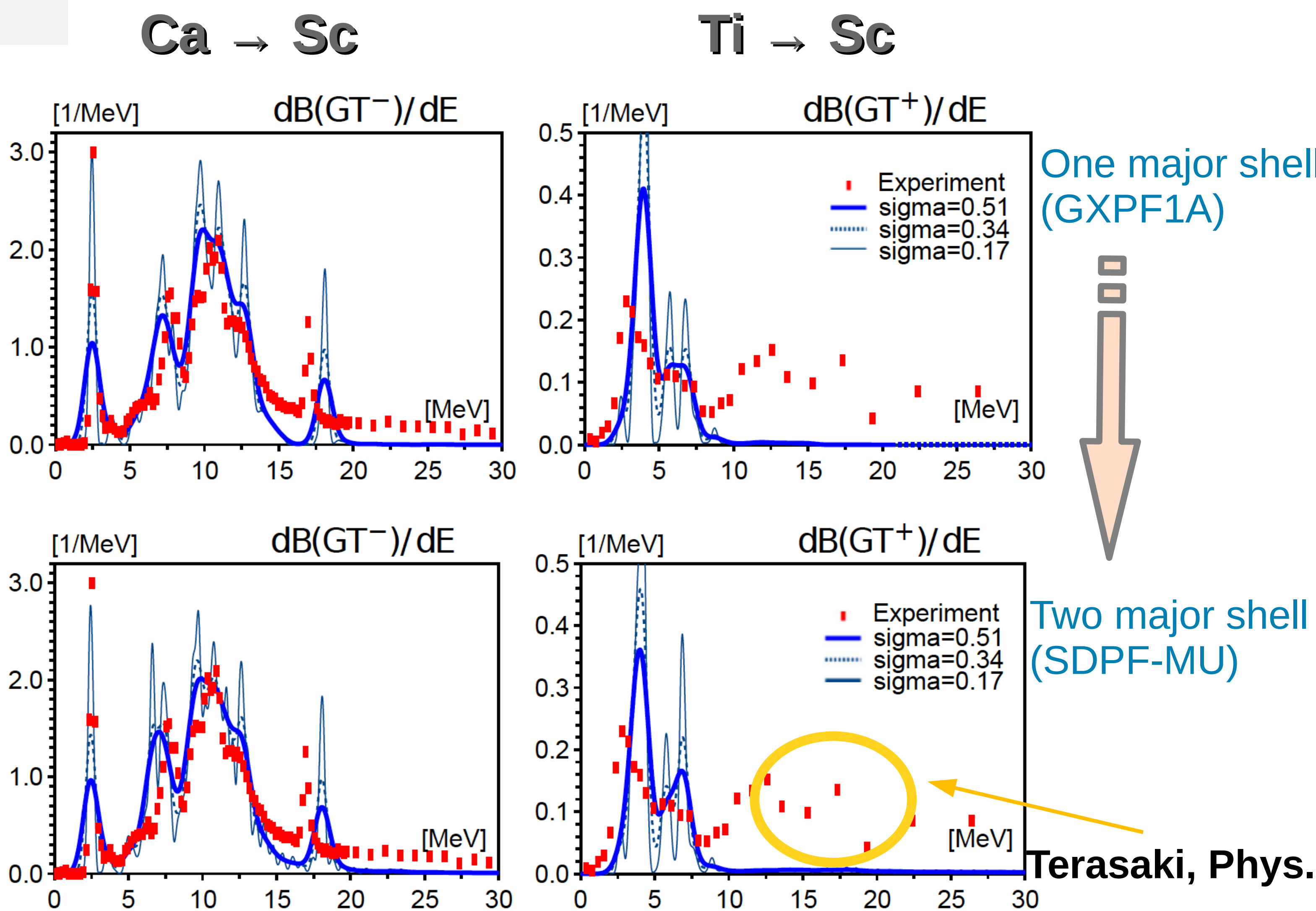

Terasaki, Phys. Rev. C 2018

Clarifies "it is IVSM"

Contribution from IVSM (isovector spin monopole) should be included in experiment. However, it is not quantitatively well known.

Y. Iwata, N. Shimizu et al. Phys. Rev. Lett. 2016

$$M^{2\nu} = \sum_m \frac{\langle 0^f_{\rm g.s.} || O_{\rm GT^-} || 1^+_m \rangle \langle 1^+_m || O_{\rm GT^-} || 0^i_{\rm g.s.} \rangle}{E_m - E_0 + Q_{\beta\beta}/2}$$

$$\overline{M^{2\nu}_+} \equiv \sum_m \frac{\sqrt{B({\rm GT}^-; m)}\sqrt{B({\rm GT}^+; m)}}{E_m - E_0 + Q_{\beta\beta}/2}$$

Inversely calculated from $T_{1/2}$

$$[T^{2\nu}_{1/2}]^{-1} = F^{2\nu} |M^{2\nu}|^2$$

NEMO3

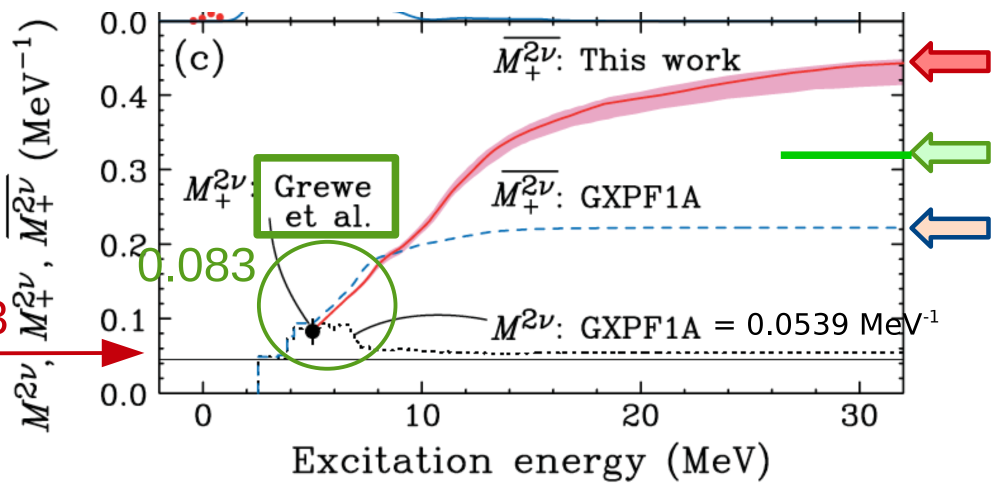

Our result

[Quenching factor]
q is determined using precise measurement
Up to Ex = 5 MeV : Grewe *et al.* PRC(2007)
q = 0.725
$M^{2\nu}$ (<5 MeV) = 0.083.

The final value of $M^{2\nu}$ is ...

SDPFMU-db calc.:

$M^{2\nu}$ = 0.0545 MeV^{-1}

$F^{2\nu}$ = 1.044 x 10^{-17} yr^{-1} MeV^6
Suhonen-Civitarese Phys. Rep (1998)

$T_{1/2}$ = 3.225 x 10^{19} yr
(100 levels of 1^+ states)

NME value in large model space

$$\left[T^{0\nu}_{1/2}\left(0_i^+ \to 0_f^+\right)\right]^{-1} = G^{0\nu} \boxed{|M^{0\nu}|^2} \left(\frac{\langle m_\nu \rangle}{m_e}\right)^2$$

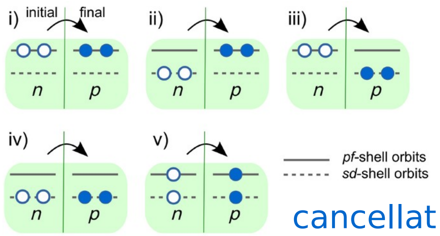

cancellation

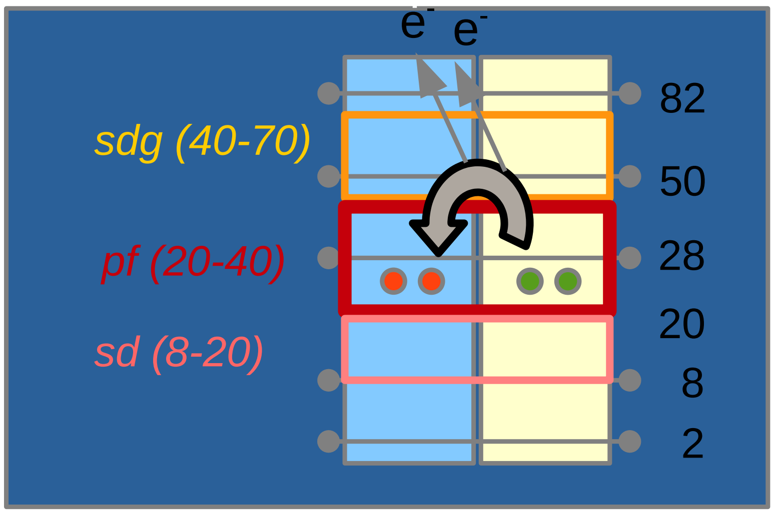

Inclusion rate of 2nd major shell components :

^{48}Ca (22%), ^{48}Ti (33%) ***sd + pf***

^{48}Ca (~2%), ^{48}Ti(~2%) ***pf + sdg***

This result shows that
It should be necessary to take into account sd shell

$M^{0\nu}$ (1 shell) 0.833

34.2 % increased

$M^{0\nu}$ (2 shells) 1.118

Due to $(1/1.34)^2 \sim 0.56$,
it means that
the half-life is almost halved
for the same neutrino mass.

Summary of NME for $0\nu\beta\beta$ of ^{48}Ca

Comparison of neutrinoless double beta decay NME (with ranges)

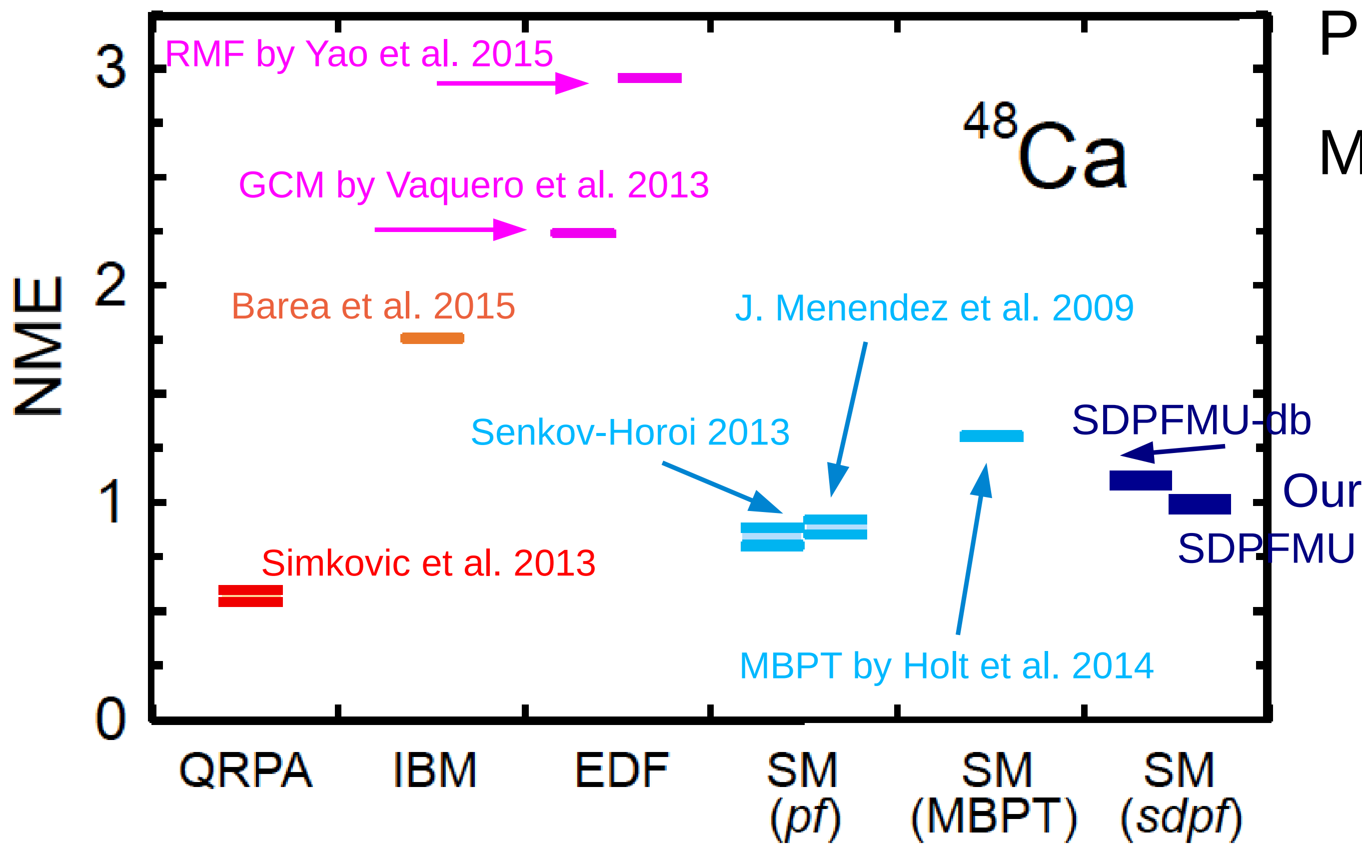

Previous GCM

$M^{0\nu} = 0.61$

Our results

Present status for DBD candidates

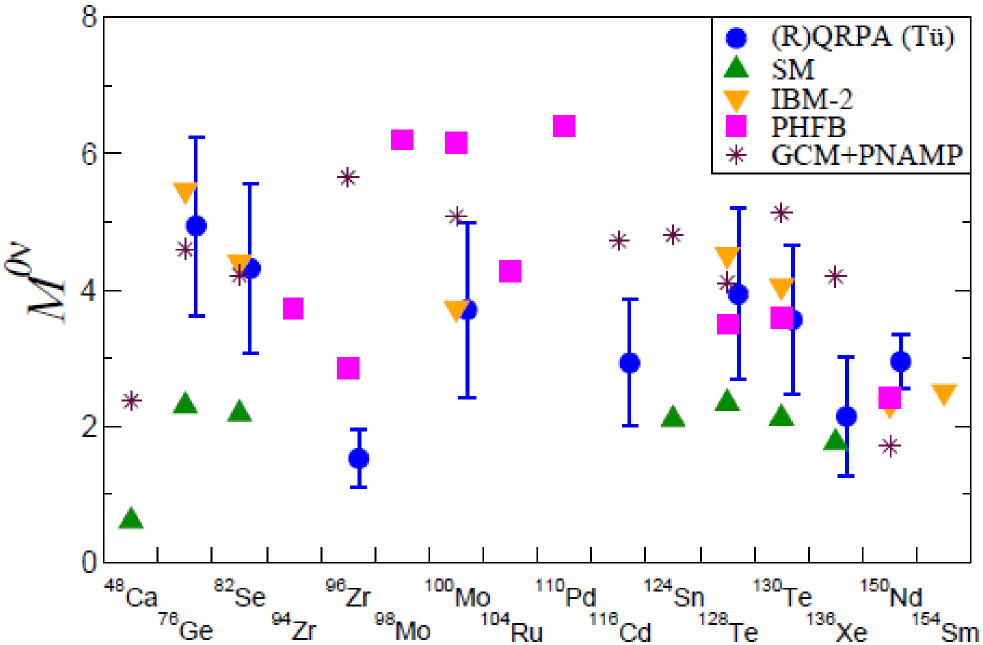

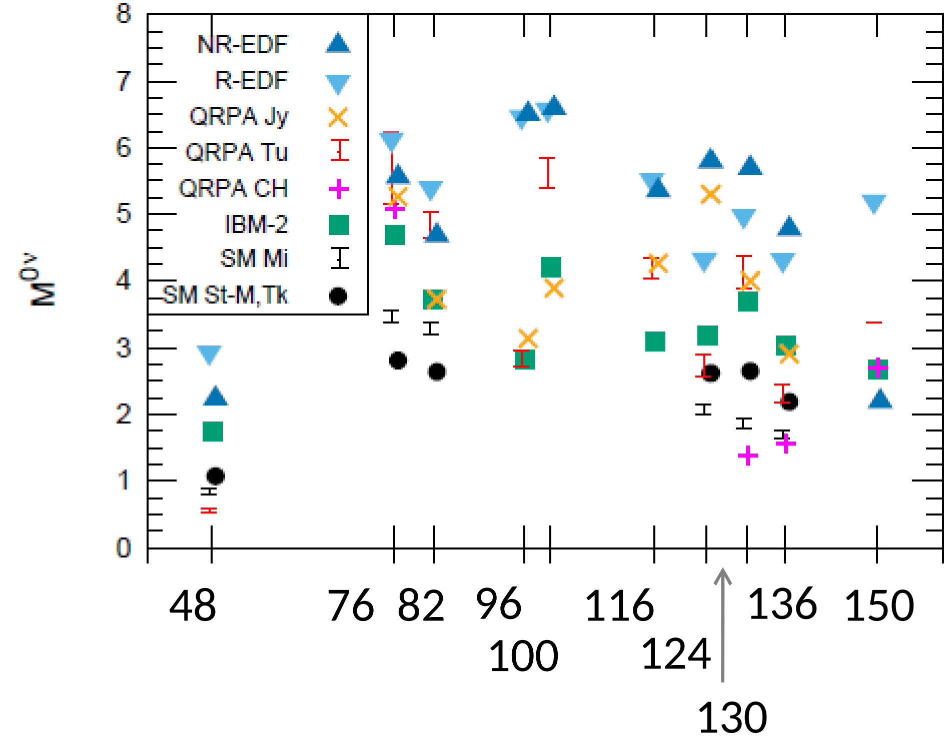

A. Feassler, J. Phys.: Conf. Ser. **337**, 012065 (2012)

J. Engel and J. Menéndez, Rep. Prog. Phys. 80 (2017) 046301

There has been **no significant difference** for these 5 years.

~ 2 to 3 times difference still exists

Reliability criterion by experiments

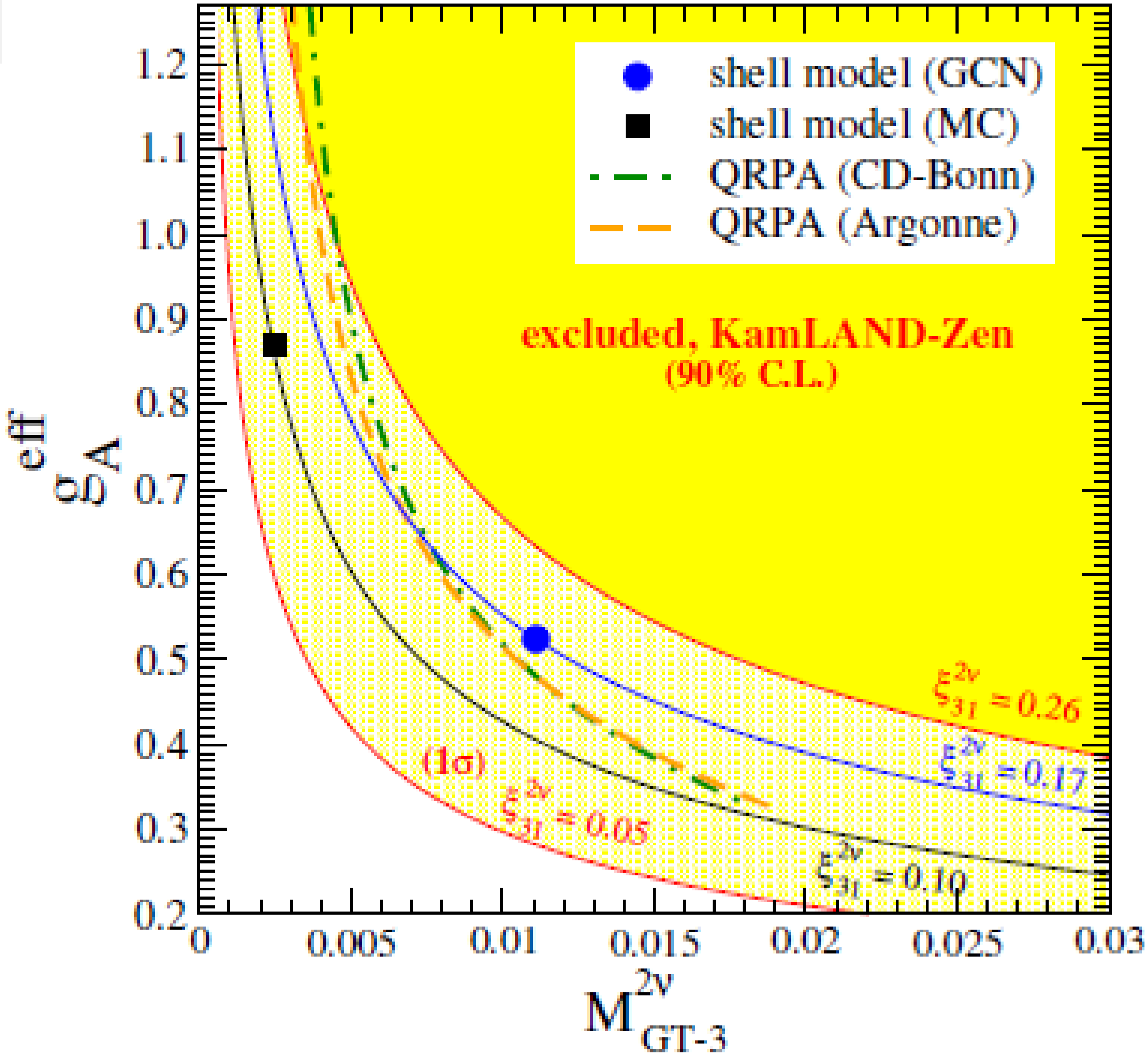

Based on
2ν experiment

Reliability of NME values by different models

Double beta decay (DBD)

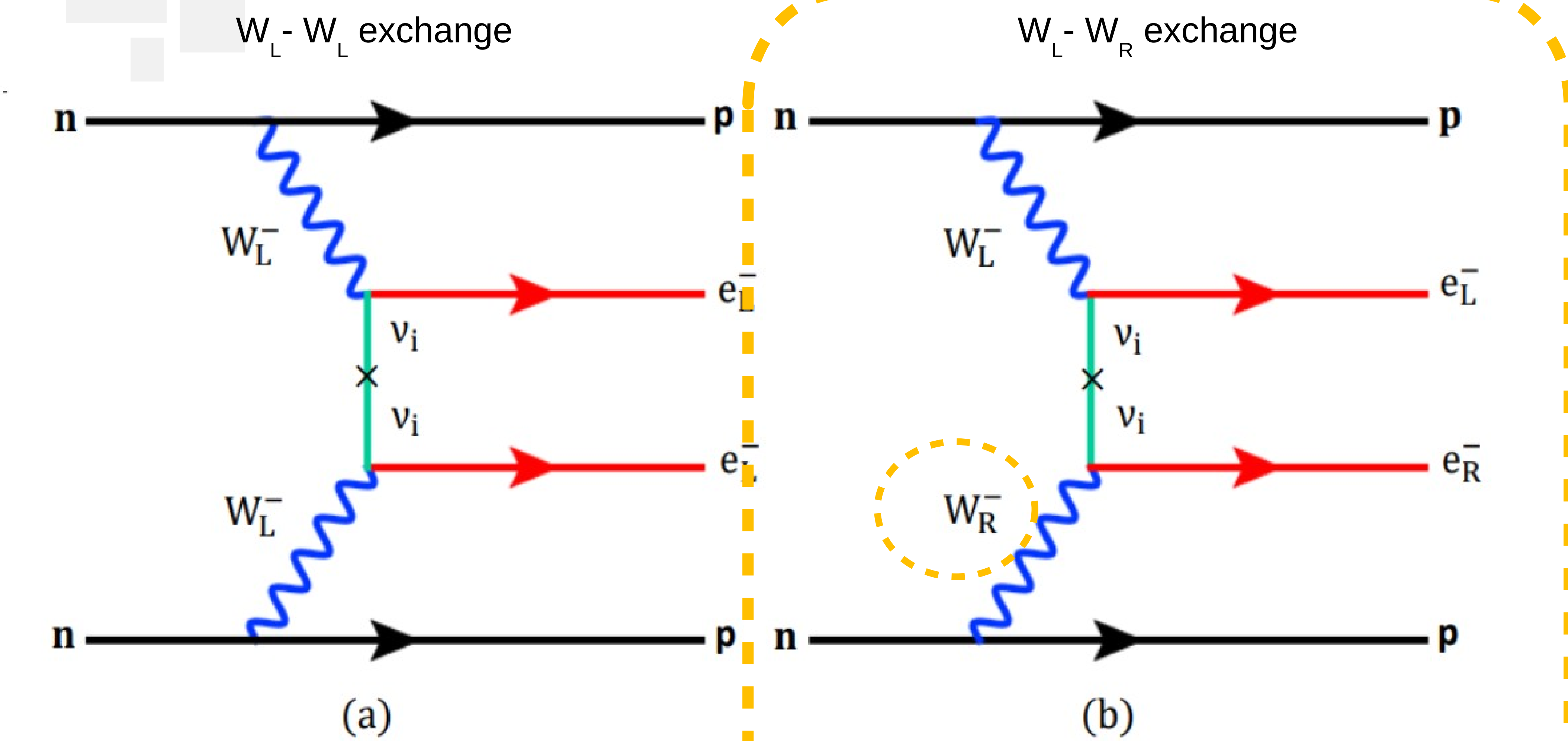

FIG. 1. (Color online) The Feynman diagrams for $0\nu\beta\beta$ via (a) $W_L - W_L$ mediation ($m_{\beta\beta}$ mechanism) and (b) $W_L - W_R$ mediation (λ mechanism) with light neutrinos exchange.

Λ mechanism

Neutrinoless DBD of ^{48}Ca

$$^{48}\mathrm{Ca} \rightarrow {}^{48}\mathrm{Ti} + e^- + e^-$$

Half life (inverse)

$$[T^{0\nu}_{1/2}]^{-1} = \underline{\eta_\nu^2 C_{mm}} + \boxed{\eta_\lambda^2 C_{\lambda\lambda} + \eta_\nu \eta_\lambda \cos\psi C_{m\lambda}}$$

usual WL-WL exchange

New

Effective lepton number violation parameters

$$\eta_\nu = \frac{m_{\beta\beta}}{m_e}, \quad \eta_\lambda = \lambda \left| \sum_{j=1}^{3} m_j U_{ej} T^*_{ej} \right|,$$

$$\psi = \arg\left[\left(\sum_{j=1}^{3} m_j U_{ej}^2\right)\left(\sum_{j=1}^{3} U_{ej} T^*_{ej}\right)\right]$$

Pontecorvo-Maki-Nakagawa-Sakata matrix

[Simkovic 2017] For Ca,

$$\eta_\nu = 2.23 \times 10^{-5}$$
$$\eta_\lambda = 2.24 \times 10^{-5}$$

[Stefanik 2015]

G_{09}	10^{-9}
G_{08}	10^{-11}
G_{07}	10^{-10}
G_{06}	10^{-12}
G_{05}	10^{-13}
G_{02}	
G_{01}	10^{-14}
G_{10}	
G_{03}	
G_{11}	10^{-15}
G_{04}	

Matrix element

$$C_{mm} = g_A^4 M_\nu^2 G_{01},$$

small~1/10 small~1/10

$$C_{m\lambda} = -g_A^4 M_\nu (M_{2-} G_{03} - M_{1+} G_{04})$$

$$C_{\lambda\lambda} = g_A^4 (M_{2-}^2 G_{02} + \frac{1}{9} M_{1+}^2 G_{011} - \frac{2}{9} M_{1+} M_{2-} G_{010})$$

large~*10 small~1/10 ~*1

accurate G_{0i}: phase space factor
(i = 1,2,3, … ,11)

$$g_A = 1.27$$

bare

Calculation of nuclear matrix element

$$M_\alpha^{0\nu} = \langle f | \tau_{-1}\tau_{-2}\mathcal{O}_{12}^\alpha | i \rangle$$

F, GT, T

$$\mathcal{O}_{12}^{GT,\omega GT,qGT} = \tau_{1-}\tau_{2-}(\sigma_1.\sigma_2)H_{GT,\omega GT,qGT}(r,E_k),$$
$$\mathcal{O}_{12}^{F,\omega F,qF} = \tau_{1-}\tau_{2-}H_{F,\omega F,qF}(r,E_k),$$
$$\mathcal{O}_{12}^{T,\omega T,qT} = \tau_{1-}\tau_{2-}S_{12}H_{T,\omega T,qT}(r,E_k),$$

$$S_{12} = 3(\sigma_1.\hat{\mathbf{r}})(\sigma_2.\hat{\mathbf{r}}) - (\sigma_1.\sigma_2), \ \mathbf{r} = \mathbf{r}_1 - \mathbf{r}_2$$

$$M_\nu = M_{GT} - \frac{M_F}{g_A^2} + M_T,$$
$$\boxed{M_{\nu\omega}} = M_{\omega GT} - \frac{M_{\omega F}}{g_A^2} + M_{\omega T},$$
$$\boxed{M_{1+}} = M_{qGT} + 3\frac{M_{qF}}{g_A^2} - 6M_{qT},$$
$$M_{2-} = \boxed{M_{\nu\omega}} - \frac{1}{9}\boxed{M_{1+}}$$

$$H_\alpha(r,E_k) = \frac{2R}{\pi}\int_0^\infty \frac{f_\alpha(q,r)qdq}{q+E_k-(E_i+E_f)/2}$$

Included:
finite nucleon size (FNS)
higher-order currents (HOC)

Four methods

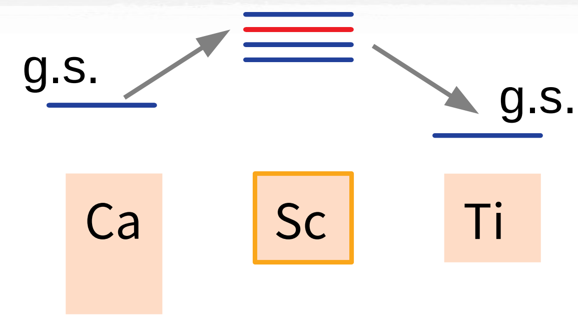

Running treatment

$$\sum_{J_k, J, E_k^* \leqslant E_c}$$

- Closure
- Running Closure
- Running non-closure
- Mixed

Closure:

$$H_\alpha(r) = \frac{2R}{\pi}\int_0^\infty \frac{f_\alpha(q,r)qdq}{q+\boxed{\langle E\rangle},}$$

Non-closure:

$$H_\alpha(r,E_k) = \frac{2R}{\pi}\int_0^\infty \frac{f_\alpha(q,r)qdq}{q+\boxed{E_k-(E_i+E_f)/2}}$$

Running closure

$$\bar{M}_\alpha^{0\nu}(E_c) = M_\alpha^{0\nu}(E_c) - \mathcal{M}_\alpha^{0\nu}(E_c) + \mathcal{M}_\alpha^{0\nu}$$

Running non-closure

Closure

Matrix elements［L-L type］

SRC = Short range correlation (短距離相関)

TABLE I. Nuclear matrix elements M_F, M_GT, M_T, M_ν for $0\nu\beta\beta$ of ^{48}Ca, calculated with GXPF1A interaction in closure, running closure, running nonclosure and mixed methods for different SRC parametrization. $\langle E\rangle = 7.72$ MeV was used for closure and running closure methods.

NME	SRC	Closure	Running closure	Running nonclosure	Mixed
M_F	None	-0.207	-0.206	-0.210	-0.211
M_F	Miller-Spencer	-0.141	-0.141	-0.143	-0.143
M_F	CD-Bonn	-0.222	-0.221	-0.226	-0.227
M_F	AV18	-0.204	-0.203	-0.207	-0.208
M_{GT}	None	0.711	0.709	0.779	0.781
M_{GT}	Miller-Spencer	0.492	0.490	0.553	0.555
M_{GT}	CD-Bonn	0.738	0.736	0.810	0.812
M_{GT}	AV18	0.675	0.673	0.745	0.747
M_T	None	-0.074	-0.072	-0.074	-0.076
M_T	Miller-Spencer	-0.076	-0.073	-0.075	-0.078
M_T	CD-Bonn	-0.076	-0.074	-0.076	-0.078
M_T	AV18	-0.077	-0.074	-0.076	-0.079
M_ν	None	0.765	0.765	0.836	0.836
M_ν	Miller-Spencer	0.504	0.505	0.566	0.565
M_ν	CD-Bonn	0.799	0.799	0.874	0.874
M_ν	AV18	0.725	0.725	0.798	0.798

Total

Matrix elements [ω type]

TABLE II. Nuclear matrix elements $M_{\omega F}$, $M_{\omega GT}$, $M_{\omega T}$, $M_{\nu\omega}$ for $0\nu\beta\beta$ of ^{48}Ca calculated with GXPF1A interaction in closure, running closure, running nonclosure and mixed methods for different SRC parametrization. $\langle E \rangle = 7.72$ MeV was used for closure and running closure methods.

NME	SRC	Closure	Running closure	Running nonclosure	Mixed
$M_{\omega F}$	None	-0.199	-0.198	-0.206	-0.207
$M_{\omega F}$	Miller-Spencer	-0.137	-0.136	-0.141	-0.142
$M_{\omega F}$	CD-Bonn	-0.212	-0.211	-0.220	-0.221
$M_{\omega F}$	AV18	-0.195	-0.194	-0.202	-0.203
$M_{\omega GT}$	None	0.66	0.659	0.766	0.767
$M_{\omega GT}$	Miller-Spencer	0.454	0.452	0.546	0.548
$M_{\omega GT}$	CD-Bonn	0.683	0.682	0.794	0.795
$M_{\omega GT}$	AV18	0.623	0.622	0.731	0.732
$M_{\omega T}$	None	-0.072	-0.069	-0.073	-0.076
$M_{\omega T}$	Miller-Spencer	-0.073	-0.070	-0.074	-0.077
$M_{\omega T}$	CD-Bonn	-0.074	-0.071	-0.075	-0.078
$M_{\omega T}$	AV18	-0.074	-0.071	-0.075	-0.078
$M_{\nu\omega}$	None	0.712	0.712	0.821	0.821
$M_{\nu\omega}$	Miller-Spencer	0.466	0.467	0.559	0.558
$M_{\nu\omega}$	CD-Bonn	0.740	0.741	0.856	0.855
$M_{\nu\omega}$	AV18	0.670	0.671	0.781	0.780

Total

The amplitude of matrix element for L-R exchange are comparable to the cases with L-L exchange.

Matrix elements [q type]

TABLE III. Nuclear matrix elements M_{qF}, M_{qGT}, M_{qT}, M_{1+}, and M_{2-} for $0\nu\beta\beta$ of ^{48}Ca calculated with GXPF1A interaction in closure, running closure, running nonclosure and mixed methods for different SRC parametrization. $\langle E \rangle = 7.72$ MeV was used for closure and running closure methods.

NME	SRC	Closure	Running closure	Running nonclosure	Mixed
M_{qF}	None	-0.102	-0.102	-0.101	-0.101
M_{qF}	Miller-Spencer	-0.082	-0.082	-0.080	-0.080
M_{qF}	CD-Bonn	-0.123	-0.122	-0.121	-0.122
M_{qF}	AV18	-0.118	-0.118	-0.117	-0.117
M_{qGT}	None	3.243	3.246	3.317	3.314
M_{qGT}	Miller-Spencer	2.681	2.684	2.751	2.748
M_{qGT}	CD-Bonn	3.554	3.557	3.709	3.706
M_{qGT}	AV18	3.423	3.426	3.502	3.499
M_{qT}	None	-0.147	-0.140	-0.143	-0.150
M_{qT}	Miller-Spencer	-0.150	-0.143	-0.146	-0.153
M_{qT}	CD-Bonn	-0.149	-0.142	-0.145	-0.153
M_{qT}	AV18	-0.150	-0.142	-0.146	-0.153
M_{1+}	None	3.937	3.898	3.989	4.028
M_{1+}	Miller-Spencer	3.430	3.389	3.480	3.521
M_{1+}	CD-Bonn	4.221	4.183	4.356	4.394
M_{1+}	AV18	4.101	4.061	4.158	4.198
M_{2-}	None	0.275	0.279	0.378	0.374
M_{2-}	Miller-Spencer	0.085	0.090	0.172	0.167
M_{2-}	CD-Bonn	0.271	0.276	0.372	0.367
M_{2-}	AV18	0.214	0.220	0.319	0.313

Total

The amplitude of matrix element for L-R exchange
are relatively large compared to the cases with L-L exchange.

Spin parity decomposition

- intermediate state -

Ca → Sc → Ti

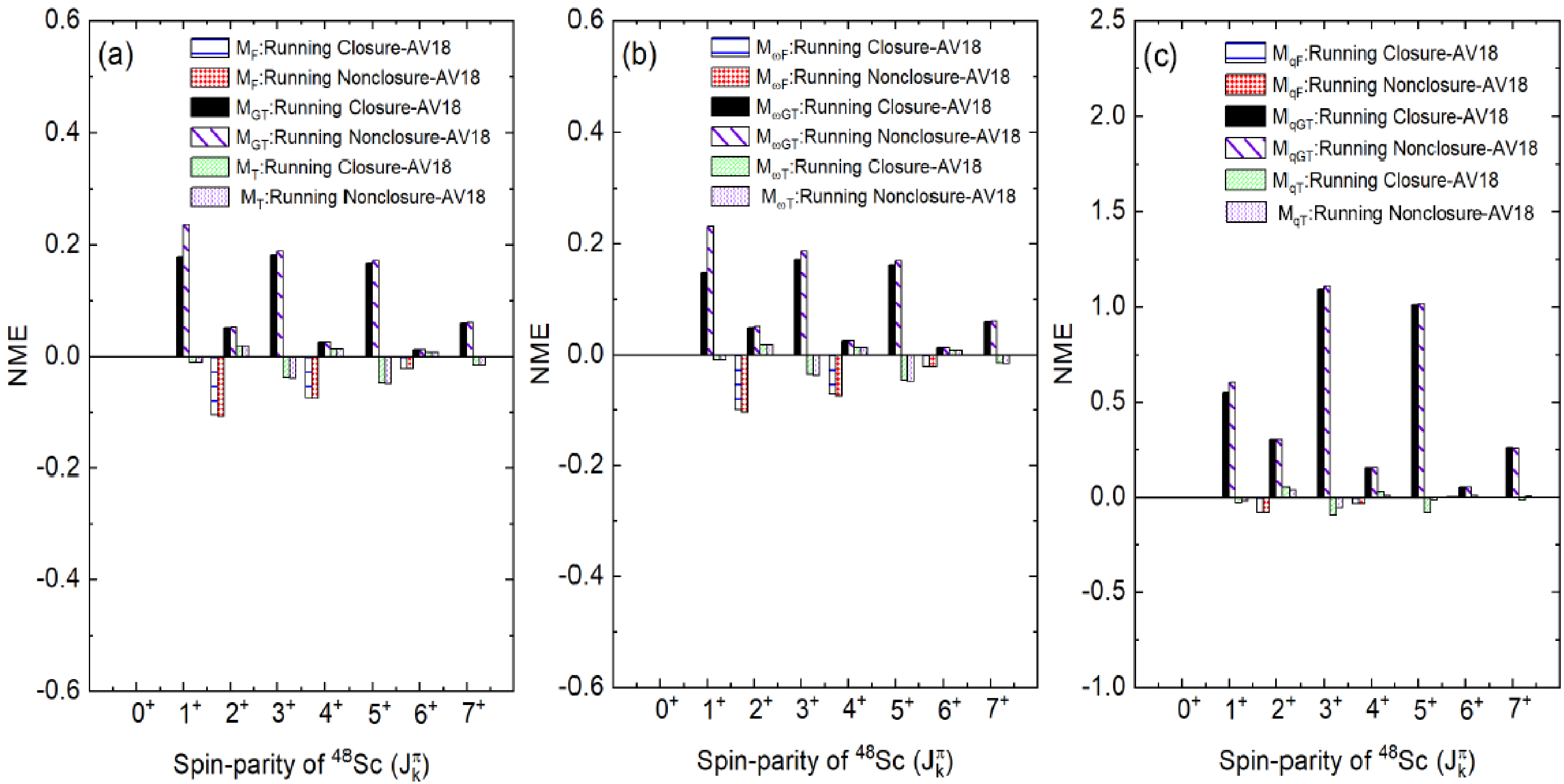

FIG. 2. (Color online) Contribution through different spin-parity of virtual intermediate states of ^{48}Sc (J_k^π) in NMEs for $m_{\beta\beta}$ and λ mechanisms of $0\nu\beta\beta$ of ^{48}Ca. Here, comparison are shown for NMEs, calculated in running closure and running nonclosure methods with GXPF1A effective interaction for AV18 SRC parametrization. $\langle E \rangle = 7.72$ MeV was used for running closure method.

Spin parity decomposition

- initial and final states -

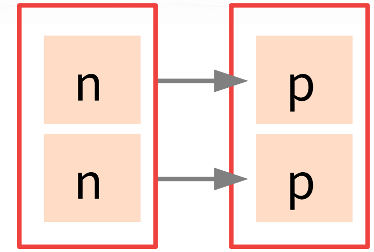

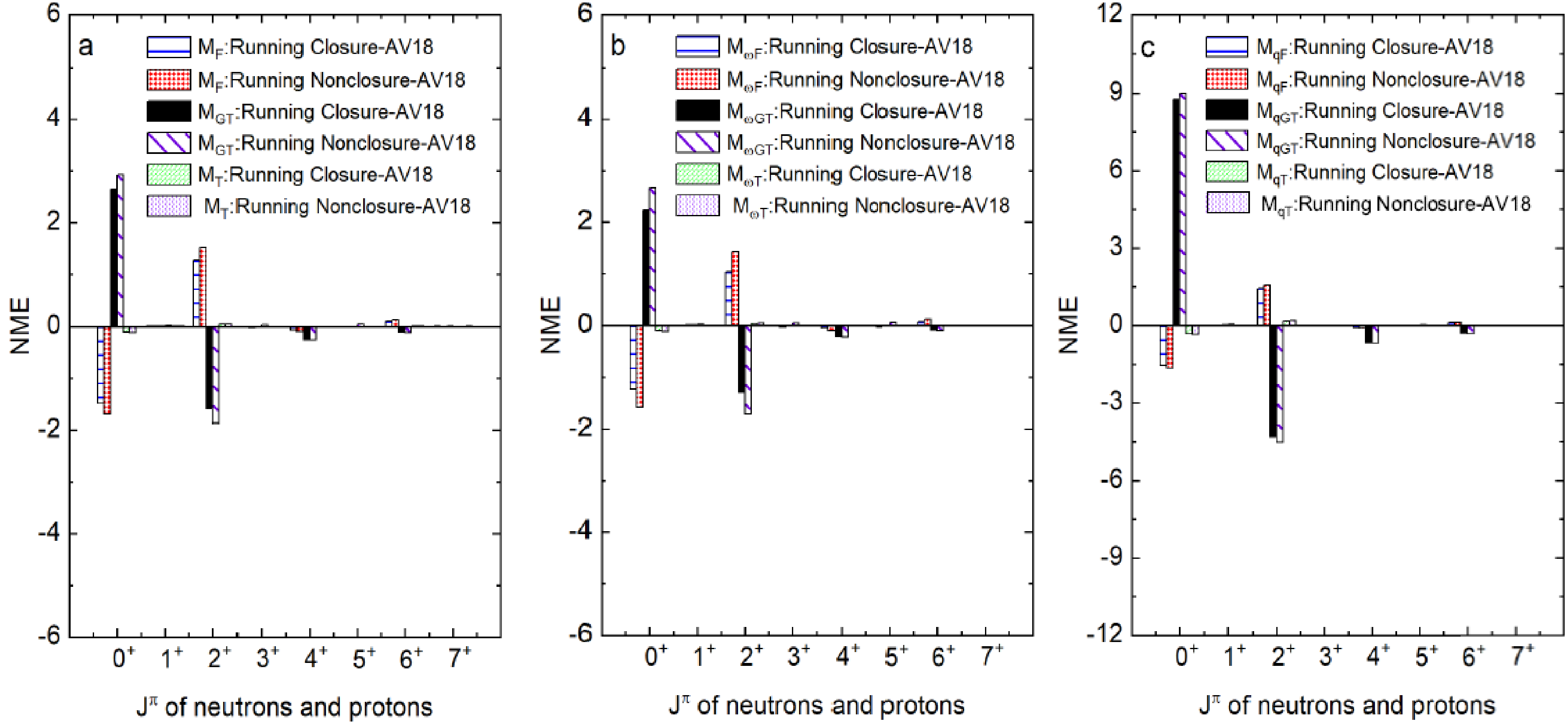

FIG. 3. (Color online) Contribution through different coupled spin-parity of two initial neutrons or two final created protons (J^π) in NMEs for $m_{\beta\beta}$ and λ mechanisms of $0\nu\beta\beta$ of ^{48}Ca. Here, comparison are shown for NMEs, calculated in running closure and running nonclosure methods with GXPF1A effective interaction for AV18 SRC parametrization. $\langle E \rangle = 7.72$ MeV was used for running closure method.

Cutoff dependence - energy -

G.S. contribution is large

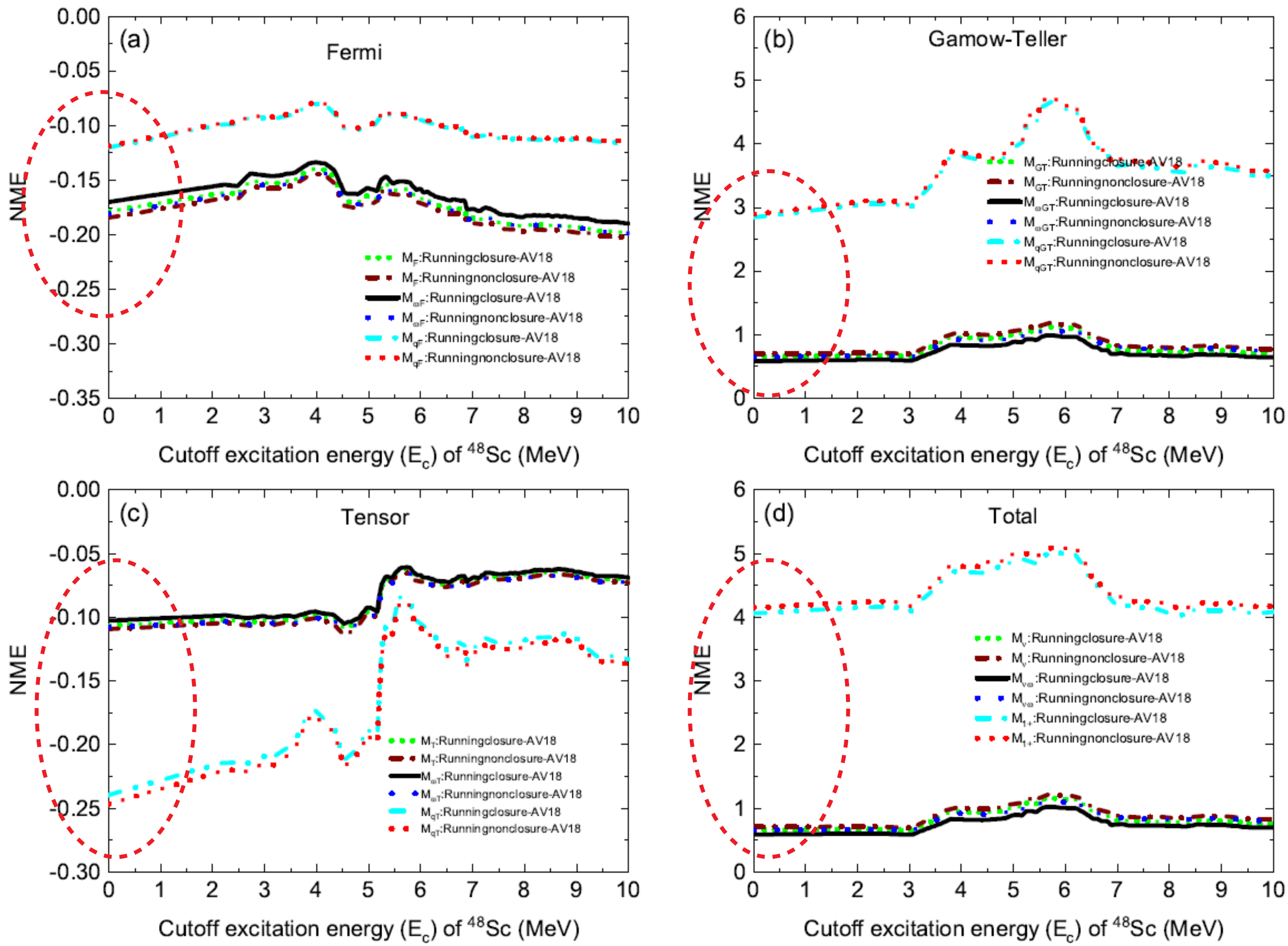

FIG. 4. (Color online) Variation of (a) Fermi (b) Gamow-Teller (c) tensor and (d) total NMEs for $0\nu\beta\beta$ ($m_{\beta\beta}$ and λ mechanisms) of ^{48}Ca with cutoff excitation energy (E_c) of states of virtual intermediate nucleus ^{48}Sc. NMEs are calculated with total GXPF1A interaction for AV18 SRC parametrization in running closure and running nonclosure methods. For running closure method, closure energy $\langle E\rangle$=7.72 MeV was used.

Cutoff dependence
- number of states -

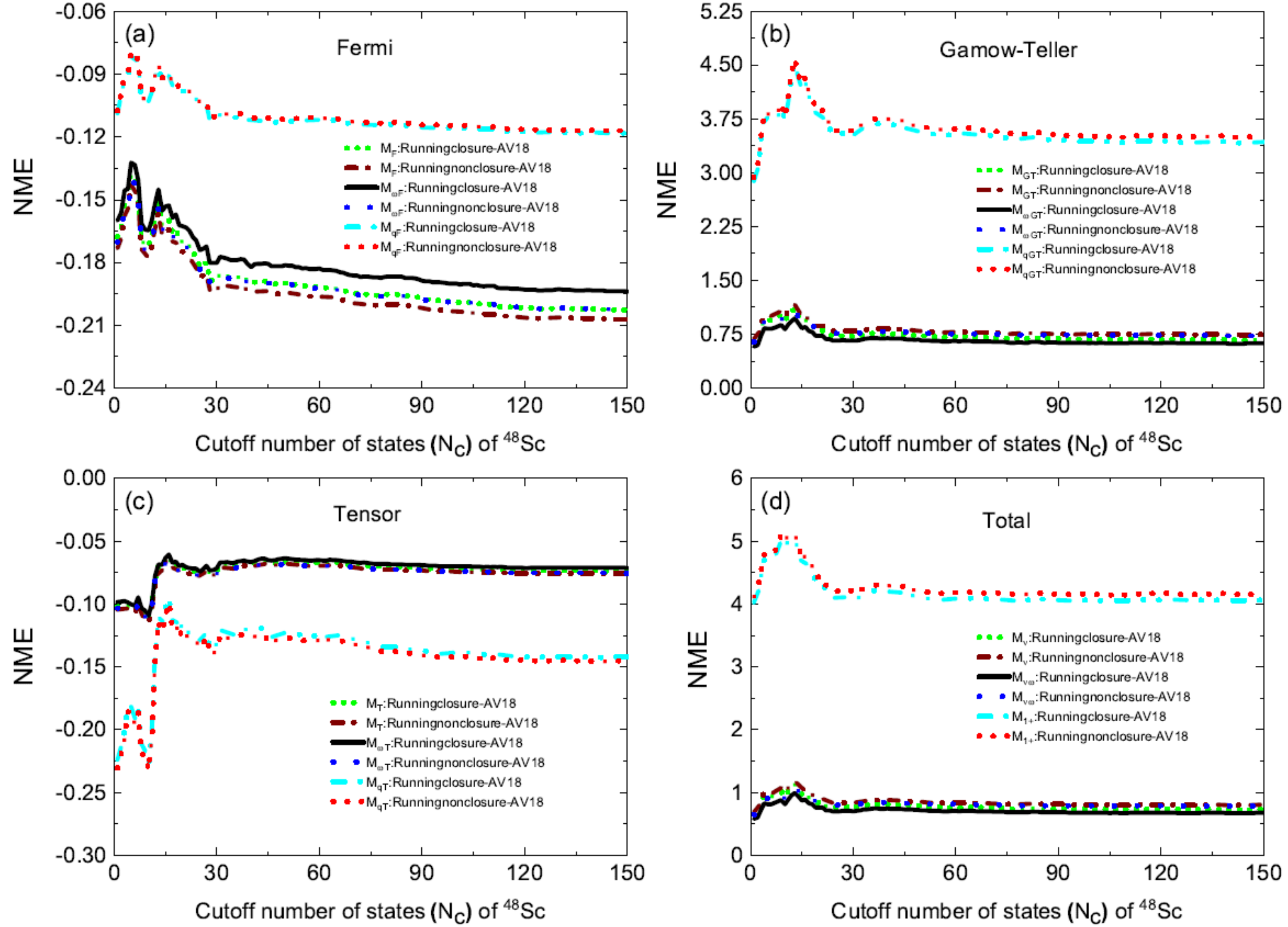

FIG. 5. (Color online) Variation of (a) Fermi (b) Gamow-Teller (c) tensor and (d) total NMEs for $0\nu\beta\beta$ ($m_{\beta\beta}$ and λ mechanisms) of ^{48}Ca with cutoff number of states (N_c) of virtual intermediate nucleus ^{48}Sc. NMEs are calculated with total GXPF1A interaction for AV18 SRC parametrization in running closure and running nonclosure methods. For running closure method, closure energy $\langle E \rangle$=7.72 MeV was used.

Closure-energy dependence

[constant] no significant change is noticed in several settings

In closure approximation

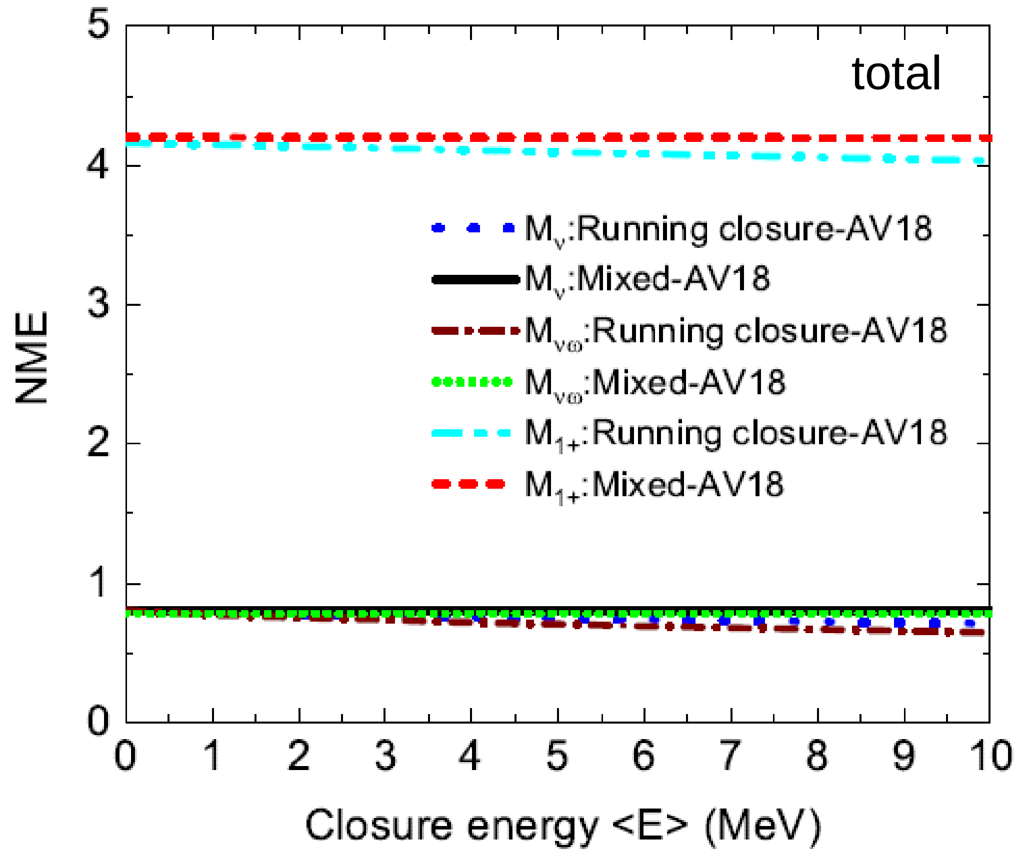

FIG. 6. (Color online) Dependence of the total NMEs for $0\nu\beta\beta$ (λ and $m_{\beta\beta}$ mechanisms) of ^{48}Ca with closure energy $\langle E \rangle$, calculated with total GXPF1A interaction for AV18 SRC parmaetrization in running closure and mixed methods.

Conclusion

$$[T^{0\nu}_{1/2}]^{-1} = \boxed{\eta_\nu^2 C_{mm}} + \boxed{\eta_\lambda^2 C_{\lambda\lambda}} + \eta_\nu \eta_\lambda \cos\psi C_{m\lambda}$$

NME	SRC	Closure	Running closure	Running nonclosure		Mixed
M_ν	None	0.765	0.765	0.836	x 1	0.836
M_ν	Miller-Spencer	0.504	0.505	0.566		0.565
M_ν	CD-Bonn	0.799	0.799	0.874		0.874
M_ν	AV18	0.725	0.725	0.798		0.798
M_{1+}	None	3.937	3.898	3.989	x 5	4.028
M_{1+}	Miller-Spencer	3.430	3.389	3.480		3.521
M_{1+}	CD-Bonn	4.221	4.183	4.356		4.394
M_{1+}	AV18	4.101	4.061	4.158		4.198
M_{2-}	None	0.275	0.279	0.378	x 1/2	0.374
M_{2-}	Miller-Spencer	0.085	0.090	0.172		0.167
M_{2-}	CD-Bonn	0.271	0.276	0.372		0.367
M_{2-}	AV18	0.214	0.220	0.319		0.313

$$C_{mm} = g_A^4 M_\nu^2 G_{01},$$

*1 (std)

$$C_{m\lambda} = -g_A^4 M_\nu (M_{2-} G_{03} - M_{1+} G_{04})$$

$$C_{\lambda\lambda} = g_A^4 (M_{2-}^2 G_{02} + \frac{1}{9} M_{1+}^2 G_{011} - \frac{2}{9} M_{1+} M_{2-} G_{010})$$

large~*10 small~1/10 ~*1

Effect should not be negligible.

$C_{\lambda\lambda}$ 1st : enlarged amplitude (*5)

$C_{\lambda\lambda}$ 2nd : comparable amplitude (*1/2)

$C_{\lambda\lambda}$ 3rd : enlarged amplitude (*2.5)

Point of discovery:

we have found
the large WR-WL effect

almost 2 times larger than WL-WL

$$g_V(q^2) = \frac{g_V}{\left(1+\frac{q^2}{M_V^2}\right)^2},$$
$$g_A(q^2) = \frac{g_A}{\left(1+\frac{q^2}{M_A^2}\right)^2},$$
$$g_M(q^2) = (\mu_p - \mu_n) g_V(q^2),$$
$$g_P(q^2) = \frac{2m_p g_A(q^2)}{(q^2+m_\pi^2)}\left(1-\frac{m_\pi^2}{M_A^2}\right)$$

$$f_{GT}(q,r) = \frac{j_0(qr)}{g_A^2}\left(g_A^2(q^2) - \frac{g_A(q^2)g_P(q^2)}{m_N}\frac{q^2}{3} + \frac{g_P^2(q^2)}{4m_N^2}\frac{q^4}{3} + \left(2\frac{g_M^2(q^2)}{4m_N^2}\frac{q^2}{3}\right)\right), \quad (15)$$
$$f_F(q,r) = g_V^2(q^2) j_0(qr), \quad (16)$$
$$f_T(q,r) = \frac{j_2(qr)}{g_A^2}\left(\frac{g_A(q^2)g_P(q^2)}{m_N}\frac{q^2}{3} - \frac{g_P^2(q^2)}{4m_N^2}\frac{q^4}{3} + \frac{g_M^2(q^2)}{4m_N^2}\frac{q^2}{3}\right), \quad (17)$$
$$f_{\omega GT}(q,r) = \frac{q}{(q+E_k-(E_i+E_f)/2)} f_{GT}(q,r), \quad (18)$$
$$f_{\omega F}(q,r) = \frac{q}{(q+E_k-(E_i+E_f)/2)} f_F(q,r), \quad (19)$$
$$f_{\omega T}(q,r) = \frac{q}{(q+E_k-(E_i+E_f)/2)} f_T(q,r), \quad (20)$$
$$f_{qGT}(q,r) = \left(\frac{g_A^2(q^2)}{g_A^2} q \boxed{+ 3\frac{g_P^2(q^2)}{g_A^2}\frac{q^5}{4m_N^2}} \boxed{+\frac{g_A(q^2)g_P(q^2)}{g_A^2}\frac{q^3}{m_N}}\right) r j_1(q,r), \quad (21)$$
$$f_{qF}(q,r) = r g_V^2(q^2) j_1(qr) q, \quad (22)$$
$$f_{qT}(q,r) = \frac{r}{3}\left(\left(\frac{g_A^2(q^2)}{g_A^2} q - \frac{g_P(q^2)g_A(q^2)}{2g_A^2}\frac{q^3}{m_N}\right) j_1(qr) - \left(9\frac{g_P^2(q^2)}{2g_A^2}\frac{q^5}{20m_N^2}[2j_1(qr)/3 - j_3(qr)]\right)\right),$$

Previous shell model calculation did not calculate/find the importance of 2nd and 3rd terms

Not calculated in
Horoi, Neascu, PRC 2018

Refs. for studying on this direction

λ-mechanism

D. Štefánik, R. Dvornický, F. Šimkovic, and P. Vogel, Reexamining the light neutrino exchange mechanism of the $0\nu\beta\beta$ decay with left-and right-handed leptonic and hadronic currents, Physical Review C **92**, 055502 (2015).

λ-mechanism (mainly by RPA calculations)

F. Šimkovic, D. Štefánik, and R. Dvornický, The λ mechanism of the $0\nu\beta\beta$-decay, Frontiers in Physics **5**, 57 (2017).

Review article (e.g. hadronic current):

J. Engel and J. Menéndez, Status and future of nuclear matrix elements for neutrinoless double-beta decay: a review, Reports on Progress in Physics **80**, 046301 (2017).

Summary

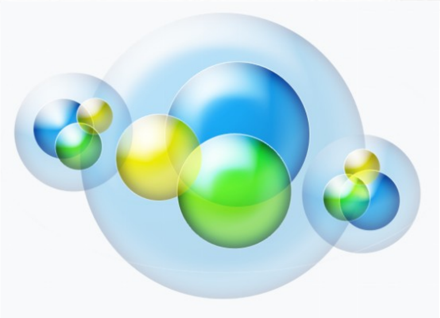

- ISM research [overview]
  + nuclear structure, + hadronic current, +ab-initio

  → **right-handed** neutrino, **right-handed** W-boson

- Shell model calculation for DBD of Ca48
  - Large scale calculation by Tokyo group -

- Right handed weak bosons ?

- (Right handed neutrino) --- sterile neutrinos ?